Methods xxx (xxxx) xxx–xxx

Contents lists available at ScienceDirect

Methods

journal homepage: www.elsevier.com/locate/ymeth

Biosensor-surface plasmon resonance: A strategy to help establish a new generation RNA-specific small molecules

Tam Vo, Ananya Paul, Arvind Kumar, David W. Boykin, W. David Wilson*

Department of Chemistry and Center for Diagnostics and Therapeutics Georgia State University, 50 Decatur St SE, Atlanta, GA 30303, USA

ARTICLE INFO

Keywords:
Biosensors biacore SPR
Drug discovery
RNA- ligand interactions
Small molecules
Heterocyclic amidines

ABSTRACT

Biosensor surface plasmon resonance (SPR) is a highly sensitive technique and is most commonly used to decipher the interactions of biological systems including proteins and nucleic acids. Throughout the years, there have been significant efforts to develop SPR assays for studying protein-protein interactions, protein-DNA interactions, as well as small molecules to target DNAs that are of therapeutic interest. With the explosion of discovery of new RNA structures and functions, it is time to review the applications of SPR to RNA interaction studies, which have actually extended over a long time period. The primary advantage of SPR is its ability to measure affinities and kinetics in real time, along with being a label-free technique and utilizing relatively small quantities of materials. Recently, developments that use SPR to analyze the interactions of different RNA sequences with proteins and small molecules demonstrate the versatility of SPR as a powerful method in the analysis of the structure-function relationships, not only for biological macromolecules but also for potential drug candidates. This chapter will guide the reader through some background material followed by an extensive assay development to dissect the interactions of small molecules and RNA sequences using SPR as the critical method. The protocol includes (i) fundamental concepts of SPR, (ii) experimental design and execution, (iii) the immobilization of RNA using the streptavidin-biotin capturing method, and (iv) affinities and kinetics analyses of the interactions using specific example samples. The chapter also contains useful notes to address situations that might arise during the process. This assay demonstrates SPR as a valuable quantitative method used in the search for potential therapeutic agents that selectively target RNA.

1. Introduction

Commercial biosensor-surface plasmon resonance (SPR) instruments became available in the early 1990s and were initially applied primarily to protein–protein (antibody) interactions due to the limited sensitivity in the beginning [1]. As instruments and software improved applications began to include protein-small molecule interactions and interest in the technology broadened. At this time the technology began to attract the attention of nucleic acid scientists interested in biomolecular interactions. In an impressive paper in 1995, Blackburn, Stockley, and coworkers quantitatively evaluated the effect of the corepressor, S-adenosylmethionine (SAM), on the interaction between the E. coli methionine repressor, and an idealized operator fragment with surface plasmon resonance on a Biacore SPR instrument [2]. DNA triple-helix formation was also followed on a Biacore instrument by Neidle and coworkers in 1995 in an early application to DNA strand equilibria [3]. Experiments to evaluate binding of small molecules to DNAs from duplexes to quadruplexes began shortly after those reports, and very quickly, Biacore instruments had been applied to double, triple and four-stranded DNA interactions with a range of compounds and macromolecules.

RNA interaction studies with a range of macro- and small molecules by SPR developed in a parallel manner to the DNA results described below. An early SPR analysis was conducted of the binding kinetics for two RNA fragments from the HIV-1 RRE RNA (Rev-responsive element) binding site that is complementary to the HIV-1 Rev protein RNA binding domain. The focus of this review is the interactions of RNA with small molecules by using SPR-based method. Early works have done by these studies which are briefly mentioned in this article. However, there are very few numbers of small molecules-RNA interactions that have been investigated by SPR compared to protein-DNA and DNA-small molecules. The smaller RBE3 RNA had an apparent equilibrium dissociation constant (K_D) of 121 nM while the larger RREIIB 41–79 RNA bound with a K_D of 2.5 nM [4]. The dissociation rates for both RNA fragments were comparable, however, the shorter sequence, RBE3, had considerably slower association kinetics. A series of known inhibitors of

* Corresponding author. P.O. Box 3965, Atlanta, GA 30302-3965, USA. Tel.: 404-413-5503.
E-mail address: wdw@gsu.edu (W.D. Wilson).

https://doi.org/10.1016/j.ymeth.2019.05.005
Received 2 February 2019; Received in revised form 15 April 2019; Accepted 4 May 2019

the Rev-RRE complex were assayed for inhibition of the RNA-protein complexes, and the results were consistent with literature inhibition constant values obtained by other methods. These results provided an early validation of the SPR method. In an important SPR study of RNA-protein interactions in 2000, Laird-Offringa, Myszka, and coworkers used SPR to investigate the binding of RRM protein motifs of the Human neuron-specific RNA-binding protein, HuD, to AU-rich elements in the 3′ untranslated regions of unstable mRNAs [5]. Complex formation resulted in stabilization of some transcripts. The results showed that a single molecule of HuD requires at least three AU rich repeat elements to bind tightly to the RNA, indicating that all three of the HuD RRM motifs are required for tight binding. The three RRM motifs cooperate not only to increase the affinity of the interaction but also to stabilize the complex.

Kissing-loop RNA-RNA interactions play important roles in many biological processes. An RNA strand interactions study by SPR involved an RNA "kissing complex." A Biacore instrument was used to determine the kinetic values for the formation of the HIV TAR-TAR* (complementary hairpin) complex [6]. The TAR component was also synthesized with 2-thiouridine at position 7 in the loop to enhance stability. The SPR results showed a very stable kissing complex with an equilibrium dissociation constant of 1.6 nM for the complex containing the modified TAR hairpin. These results illustrate the power of the SPR method to investigate RNA strand equilibria. A SELEX procedure was used to obtain a new kissing-loop RNA motif that could also bind the HIV-1 trans activation (TAR) RNA. SPR analyses were used with this RNA motif and showed strong kissing loop-loop interactions. Unexpected differences were observed in the divalent cation dependency of the interactions and illustrate the use of SPR in the analysis of RNA-ion interactions.

Small molecule RNA interaction studies by SPR began to appear in this time period. Even though there are fewer compounds for selective RNA than for DNA binding SPR has been used extensively for RNA-small molecule analysis. Starting in the late 1990s Wong and coworkers published an impressive series of papers on aminoglycosides (AG) and related compounds binding to different RNAs from aptamers to ribosome A-site models [7]. In another very early study, the Wong group used SPR to evaluate the specificity of neomycin B and related aminoglycoside antibiotics (Fig. 1) for interaction with the Rev-responsive element (RRE) of HIV-1 mRNA and some analogs [8]. They found in an analysis of neomycin B binding with three short synthetic RRE RNA hairpin models that the compounds had submicromolar binding affinity and 1:1 stoichiometry in each case. This and related results suggest that neomycin B may generally bind with this affinity to regular A-form RNA or hairpin loops with little selectivity [9]. Work on development of AGs to selectively target RNA, and the A-site, in particular, has continued to the present day with a number of different AG synthetic modifications. The original compounds were nonselective, but several of the modification types have improved the selectivity. A library of diverse AG derivatives was screened with SPR against RNA hairpin models of the bacterial A-site, and the HIV viral TAR and RRE sequences. Interestingly, the screen showed that the same four aminoglycoside derivatives bound most tightly to all three of the RNAs [10]. Unfortunately, the compounds in this study that are good RNA binders discriminate poorly among different RNA sequences. In further studies selected aminoglycoside derivatives and the RNA hairpins were studied in more detail using an SPR assay. Three isomeric AGs from the initial screen were found to bind tightly to the RNA hairpins (with K_D values from 0.23 to 4.7 μM). The strongest RNA–aminoglycoside interactions arise primarily from slow dissociation of the AGs from the RNA targets. The three tight-binding derivatives were also found, however, to discriminate poorly among alternative RNA sequences, as observed in several other AG studies [10]. These SPR results illustrated that more selective binding small molecules would be needed for RNA applications in general.

Totally different compounds were found in a major effort to design RNA targeted HIV-1 therapeutics by RiboTargets Ltd in England [11]. The results showed a strong interaction with a TAR model system by a bis-guanidine compound, rbt203 and its analogs by fluorescence, NMR, molecular modeling and SPR. The compound induced a conformation in TAR similar to that brought about by the Tat protein. Several SPR studies of small molecule interactions with RNA G-quadruplexes have recently appeared and this area, no doubt, will continue to grow in the near future with a strong possibility of development of compounds specific for RNA quadruplexes [12].

In the 1990s time period, our laboratory was developing a library of heterocyclic amidines to target the DNA minor groove as antiparasitic agents [13]. As part of a search for therapeutic organic compounds that selectively target RNA in the compound library, specific diphenylfuran derivatives (Fig. 1), which are related to compounds that bind to the

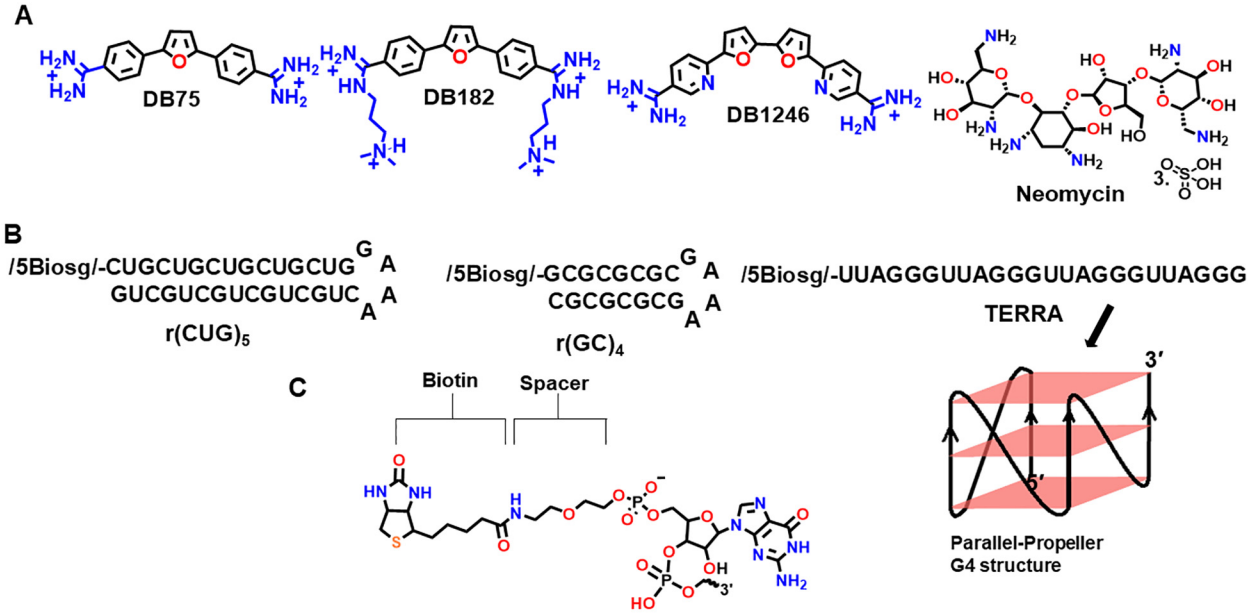

Fig. 1. (A) Structure of some heterocyclic diamidine RNA binders and Neomycin; (B) 5′-biotin-labeled RNA example sequences used in this study; (C) Structure of the 5′-RNA biotin derivative nucleotide used during immobilization.

DNA minor groove, were found to bind very strongly to RNA in a manner that is sensitive to the structure of the compounds [14]. Based on the recognition of the A-site and other RNAs by AGs, we extended several diamidine compounds with alkylamine functions (For example, DB182 in Fig. 1) to give tetracations. In more detailed studies of DB340 the best binding compound of the series, we found that the DB340 tetracationic heterocycle, which contains a phenyl-furan-benzimidazole unfused core aromatic system, exhibits pronounced selectivity for the RRE RNA stem-loop from HIV-1 [15]. NMR results indicated that DB340 binds to the RRE duplex minor groove in a highly structured and cooperative complex at a 2:1 DB340 to RRE ratio. Additional studies with mutant RRE sequences indicate that the internal loop of RRE is required for strong, specific binding of DB340, as also observed with the Rev protein (14). The Tor laboratory used a fluorescence assay to investigate the same compounds (including DB182 in Fig. 1) for binding to a larger RRE model system [16]. They found that both DB340 and DB182 bound strongly to the RNA with DB340 binding stronger in agreement with the SPR results. As with the AGs, SPR studies on the heterocyclic amidine compounds are also continuing with design and development of new compounds.

An impressive and important series of SPR studies on RNA interactions with synthetic compounds from their laboratory have been conducted by Nakatani and coworkers. They used SPR analysis as part of a method to discover compounds that bind to different RNAs as part of a therapeutic development project. In 2006 they designed agents to target the RNA stem-loop IIB of RRE of HIV-1 as potential therapeutic agents for HIV-1 infection [17]. The IIB loop is characterized by consecutive G-G and G-A mismatches and is the binding site for the Rev protein which is primarily responsible for nuclear export of viral mRNA. They designed bifunctional ligands with groups for binding to both Gs and the G and A in the G-G and G-A mismatches in the internal loop in competition with Rev peptide. The results were quite successful, and SPR analysis indicated that the compounds bound well and caused the dissociation of a pre-formed Rev–RRE complex in a model system [17]. Related compounds that did not bind the mismatches were inactive. Development of additional compounds in this area is promising for targeting mismatches which are quite common in biologically important RNAs.

The maturation process of microRNA (miRNA) production was developed as a metabolic path for drug-targeting to modulate the expression of genes related to a number of diseases [18–19]. Discovery studies for small molecules that bind to the precursor of miR-29a (pre-miR-29a) were conducted on a library containing over 40 thousand compounds by a fluorescent indicator displacement (FID) assay [20]. The assay identified over one thousand hit compounds, which were subsequently evaluated in an SPR assay on a pre-miR-29a immobilized surface. Over 20 hit compounds, which had not been reported previously to bind to RNA were identified. To gain more information on the motif structures that favor binding to pre-miR-29a, 19 substructures were selected from the hit compounds. The substructure library consisted of 362 compounds from the original library. An SPR assay of this library on a pre-miR-29a-immobilized surface indicated that five substructures could potentially be important structural motifs for pre-miR-29a interaction [20]. The results provided SPR experimentally validated compounds with both affinity and kinetics information for targeting pre-miRNAs.

The Nakatani group has also investigated compounds to target the r(CUG) repeats that cause the neurological disorder myotonic dystrophy type 1 (DM1) [21,22]. The pathological features of DM1 include the formation of ribonuclear foci containing expanded r(CUG) repeats (Fig. 1), which sequester the MBNL1 protein and lead to the misregulation of alternative pre-mRNA splicing [21]. Several groups are successfully working on the discovery of small molecules that bind to the r(CUG) repeats and improve alternative splicing with therapeutic potential in the treatment of DM1 [21–24]. The Nakatani findings are described here since they have extensively used SPR methods in the discovery process. They have shown that the synthetic compound 2,9-diaminoalkyl-1,10-phenanthroline (DAP) is an attractive candidate for binding to the repeated UU mismatch core unit in CUG repeat RNA [21,22]. In recent studies, they have synthesized a dimeric form of DAP, DDAP in an effort to enhance the CUG repeat RNA binding [22]. Their SPR assay along with other methods confirmed the binding of DDAP to $r(CUG)_9$ repeats. The success of the discovery was confirmed in a DM1 cell model and a DM1 mouse model which showed effective recovery of the pre-mRNA splicing defects on treatment with DDAP. Their studies indicate that DDAP could interfere with the binding of MBNL1 to r(CUG) repeats. Again, SPR studies were a key feature of the development of these new RNA binding compounds and provided extensive information about the interactions. Similar syntheses and discovery studies are continuing in the Nakatani laboratory.

In other recent studies, Sugiyama and coworkers have used SPR to investigate the RNA binding properties of some very different compounds, pyrrole-imidazole (PI) polyamides with which they have extensive experience [25]. They designed PI polyamides that target rat transforming growth factor-β1 (TGF-β1 polyamide) and influenza A virus (PA polyamide) and analyzed RNA binding properties of the polyamides. Biacore binding assays showed binding of the TGF-β1 polyamide to the RNA target, but a mismatch polyamide did not bind. Although the PA bound strongly to the RNA, it bound with a significantly higher K_D than with DNA which was primarily due to a fast dissociation rate from the RNA [25]. This type of kinetics information, which is readily available in biosensor-SPR studies, illustrates a major advantage to using SPR in analysis of RNA and DNA complexes. A PI polyamide was also designed to target the influenza A virus RNA. The polyamide was found to have a K_D value of 460 nM for targeting the dsRNA of influenza A virus. Although the current polyamides bind much more strongly to DNAs that similar RNAs, they illustrate the potential for pursuing a modified PA design for RNA targeting.

It should be emphasized that the studies described above are just the "tip of the iceberg" of the discovery of new compounds for targeting RNA for biotechnology and potential therapeutic applications [some recent review examples, [26–30]]. Work in academic and company laboratories is proceeding rapidly on synthetic RNA binding agents. A number of new companies have been started, and a significant amount of money is being invested in developing new RNA targeted therapeutics. What distinguishes the studies described above is that they all use SPR as part of the discovery process. Other groups have also discussed several different applications of SPR and SPR Imaging for biomolecules interactions [31–34]. Only a part of the papers on SPR of RNA interaction studies could be presented, but these illustrate the exciting discoveries that are being made with the important assistance of the information from SPR analyses. It is expected that SPR will continue to play a major role in future discoveries of new and improved RNA binding agents where there is a need for affinity, kinetics and stoichiometry information in the discovery process.

1.1. Basic principles of biosensor-SPR methods

A biosensor experiment starts with immobilization of one of the reaction components on a selected flow surface in a manner that does not significantly perturb its ability to bind to other reaction components. Either the RNA or another reaction component can be immobilized. Reaction components, that are not immobilized, are dissolved in an appropriate buffer, of which there are many (see Section 2.4.1). All of these steps and equipment are described in detail below. The results of a biosensor-SPR experiment, flow of one or more reaction components over the surface with the immobilized reaction component, are typically presented as a series of sensorgrams. In a sensorgram, the SPR binding signal (such as response units or RU in Biacore and some similar designation in other instruments) is shown as a function of time (Fig. 2C). A common material for the flow surface is carboxymethyl dextran or a similar material (Table 1). The surface can be used for

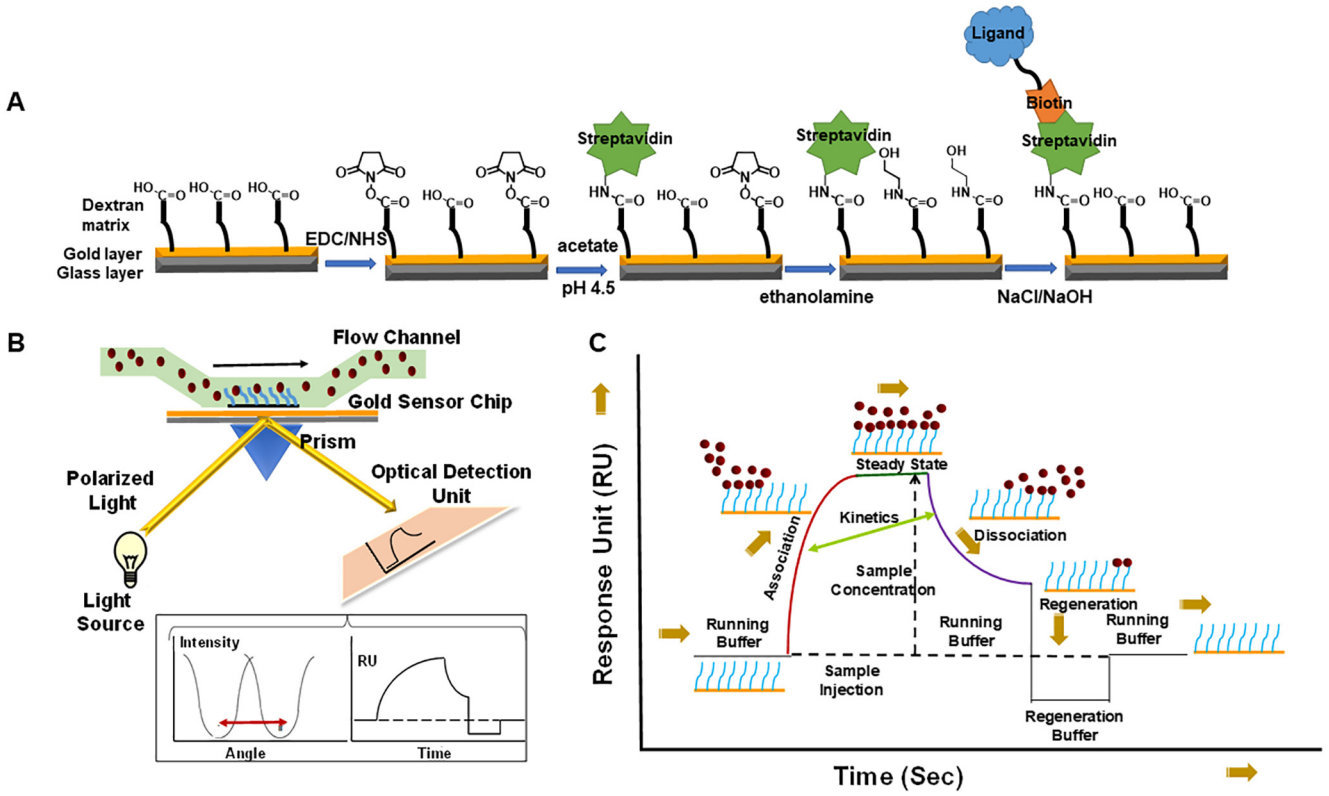

Fig. 2. (A) The procedure for the immobilization of 5′-biotin labeled RNA on CM5 Chips; (B) Schematic representation of biomolecular interactions observed in a flow cell and SPR angle change with some of the critical components labeled; (C) SPR sensorgram and its components described in steps.

direct covalent attachment of proteins, RNA, DNA, or noncovalent capture of a nucleic acid strand with biotin linked to either the 5′ or 3′ terminus, Fig. 2A (*see* Section 2.3 for more detail about immobilization). The terminal attachment of biotin, through a flexible linker (Fig. 1C), leaves the nucleic acid binding sites open for complex formation with no significant perturbation of the binding site(s). A range of other sensor chips surfaces and immobilization chemistries are also available, and it is generally possible to find an appropriate surface for essentially any biological interaction application (Table 1, *see* Note 1). Any appropriated functionalized small molecule can also be immobilized but this is generally more difficult to do without perturbation of binding of the small molecule. In the biosensor-SPR experiments presented as part of this review 5′-biotin-labeled RNA sequences (Fig. 1B) such as $r(CUG)_5$, $r(GC)_4$, Human Telomeric RNA G-quadruplex folded sequence (TERRA) (full sequences in Fig. 1B) were used. The general immobilization strategy is to preserve the structure and function of the immobilized ligands. It is vital to know the general structure of the ligands to ensure that the immobilization site does not perturb the active binding site of the ligand. For example, we found that it works best for RNA and DNA to have the biotin covalently attached to the 5′ side of the hairpin or a complementary strand, and the preferred attached site is the guanosine or cystine. This biotinylated strategy ensures the nucleic acid structure remains intact after immobilization and prevents any perturbation that might happen at the active binding site of RNA. In principle 3′-biotin attachment should work in cases where such attachment is an advantage. The same principle can be

Table 1
Example of different types of chips (available from GE Healthcare Inc.)

Type	Features	Use
C1	Carboxymethylated, matrix-free surface for covalent immobilization	Need to avoid dextran on the surface for multivalent or very large macromolecules
CM3	Similar properties to sensor chip CM5, suited to large interaction partners and exploratory assay conditions	The interaction partner in solution is very large and exploratory assay conditions
CM7	Similar properties to sensor chip CM5, but for fragment and low molecular weight molecule samples with three times higher capacity	Suitable for work with small molecules and fragment-based screening when achieving the required immobilization level is challenging
SA	Carboxymethylated dextran pre-immobilized with streptavidin for immobilization of biotinylated interaction partners	High binding capacity, reproducibility and chemical resistance give excellent performance over a broad range of applications.
HPA	Flat hydrophobic surface consisting of long-chain alkanethiol molecules is attached directly to the gold film. It facilitates the adsorption of lipid monolayers for analysis of interactions involving lipid components	Model membrane systems
L1	Lipophilic groups are covalently attached to carboxymethylated dextran, making the surface suitable for direct attachment of lipid membrane vesicles such as liposomes.	High-capacity capture of vesicles and liposomes while maintaining the lipid bilayer
NTA	Carboxymethylated dextran pre-immobilized with nitrilotriacetic acid (NTA). Histidine-tagged molecules are immobilized via Ni2+/NTA chelation.	Capture and immobilization of histidine-tagged molecules via metal chelation
Protein L	Carboxymethylated dextran matrix pre-immobilized with a recombinant Protein L for antibodies and antibody fragments containing kappa light chain subtypes (1, 3 and 4) without interfering with its antigen-binding site	Oriented capture of antibody fragments

Table 2
Biacore instrument commands.

Biacore Control Software commands	Function
Desorb	Removes adsorbed materials from the flow system
Sanitize	Removes disinfects from the flow system
Superclean	Washes the flow system and denatures proteins to increase their solubility
Prime	Flushes the flow system with running buffer
Dock	Docks the sensor chip into the instrument
Undock	Undocks the sensor chip from the instrument
Manual Run	Allows to control a run interactively
Sample Injection	Injects Sample
Kinetics/Affinity	Start a kinetics or affinity evaluation from the Biaevaluation software

applied to larger biological systems such as proteins or antibodies that have been studied elsewhere [35]. The advantage of SPR is the diversity in different immobilization methods that have their own advantage in specific systems. It is best if the binding capacity, affinity and kinetics can be tested with a well-characterized compound from solution studies.

The SPR experiment can be performed in a series of single kinetic injections. To start the experiment a reference baseline is initially established by buffer flow over the immobilized RNA surface and secondly, a solution of immobilized reaction components, such as a small molecule, are injected over the surface with the immobilized reactant. Binding to the RNA is monitored by changes in the SPR signal based on the change in refractive index at the sensor surface of the solution upon complex formation (Fig. 2B). With sufficient injection time, a steady-state plateau, where association and dissociation of the complex are occurring at an equal rate, is established (Fig. 2C). Finally, buffer flow (without ligand) is reinitiated and the dissociation of the complex is monitored as a function of time. The above steps describe a single kinetic injection and are repeated with a series of concentrations of the flow component(s) (Fig. 2C). The resulting sensorgrams are fitted to an appropriate binding model as described below. Example sensorgrams for an RNA-small molecule interaction are shown in data analysis and result section.

For a ligand (L) binding to a site on an RNA sequence/structure and forming a single complex (C), the interaction is described by the following equation:

$$\mathrm{L} + \mathrm{RNA} \underset{k_d}{\overset{k_a}{\rightleftharpoons}} \mathrm{C} \tag{1}$$

and the equilibrium binding affinity for this interaction is:

$$K_A = \frac{[\mathrm{C}]}{[\mathrm{L}][\mathrm{RNA}]} = \frac{k_a}{k_d} = \frac{1}{k_D} \tag{2}$$

where [L] is the concentration of the injected ligand, [RNA] is the concentration of the immobilized RNA not bound to the ligand (free RNA concentration), and [C] is the concentration of the complex, bound RNA and ligand; K_A is the equilibrium binding constant, k_a is the association rate constant and k_d is the dissociation rate constant.

For association:

$$\frac{d[\mathrm{C}]}{dt} = k_a[\mathrm{L}][\mathrm{RNA}] + k_d[\mathrm{C}] \tag{3}$$

and for dissociation:

$$-\frac{d[\mathrm{C}]}{dt} = k_d[\mathrm{C}] \tag{4}$$

Both the association and dissociation phases of the sensorgram can be simultaneously fit to a desired binding model with several sensorgrams at different ligand concentrations using a global fitting routine [36,37]. Global fitting allows the most robust determination of kinetic constants (k_a or k_d) and the calculation of equilibrium constants, K_A or K_D, from the ratio of kinetic constants (Eq. (2)). If a steady-state plateau is obtained, the SPR response in the plateau region, can be used with the following model to obtain the equilibrium constant:

$$r = \frac{K_A C_{free}}{1 + K_A C_{free}} = \frac{RU_{obs}}{RU_{max}} \tag{5}$$

for the 1:1 binding model described above.

In this model r represents the moles of bound ligand per mole of RNA total and C_{free} is the free ligand concentration in equilibrium with the complex. Note that an advantage of this experiment is that C_{free} is constant because of the flow of non-immobilized reaction components. RU_{obs} is the observed (experimental) response in the plateau region and RU_{max} is the predicted maximum response for a one ligand binding to an RNA site. RU_{max} can be calculated or determined experimentally at the RU for saturation of the RNA binding sites by the equation:

$$\frac{RU_{max}}{RU_{RNA}} = \frac{MW_{compound}}{MW_{RNA}} \tag{6}$$

For a 1:1 binding interaction, the RU_{max} can be calculated from the known molecular weight (MW) of compound and RNA, and the immobilized RU value of RNA as in Eq. (6). RU_{max} is for 1:1 binding but in cases where there is more than one binding site on the RNA, the RU_{sat} at saturation binding will be $> RU_{max}$. The beauty of stoichiometry in SPR is that RU_{sat} can be equal to RU_{max}, or equal to ($n \times RU_{max}$) where n = 2, 3, 4 … molecules This is because each compound in an SPR method gives the same RU for binding.

If the compound dissociates from RNA-ligand complex rapidly with complete dissociation, then no regeneration reagent is needed. In many cases an ionic buffer like 1 M NaCl or KCl as a regeneration buffer can be used for complete dissociation of the ligand from the RNA. However, If the complex binds strongly and dissociates slowly, the surface can be regenerated before the complete dissociation occurs with a solution that causes rapid dissociation of the ligand without irreversible damage to the immobilized RNA [*see* Note 9 and Table 3] [37,38]. For example, a solution at pH (pH ≤ 4) can briefly unfold RNA and cause the ligand to dissociate completely. Additional injections of the running buffer (around neutral pH) allow the immobilized RNA to refold and establish a stable baseline. This cycle is repeated with a series of additional ligand concentrations with a series of sensorgrams generated with a broad range of concentrations, both the kinetics and equilibrium constant can be determined as discussed above.

We recommend using a strong ionic buffer as the first choice for regeneration buffer, based on the ability to keep the RNA folded and intact with compete dissociation of the bound compound from the RNA. Since the RNA chemical stability in the unfolded state is less than an analogous DNA, some solutions, such as strong bases, which can cause the deprotonation of the 2′–OH, cannot be used with RNA.

Table 3
Regeneration solutions.

Interaction Strength	Acidic	Ionic
Recommended	pH ~ 3 10 mM Glycine/HCl HCl formic acid	1 M NaCl 1 M KCl (higher concentration of NaCl and KCl can be used)
Can be used for difficult regeneration (brief injection < 60 sec)	pH 2–2.5 10 mM Glycine/HCl formic acid HCl H_3PO_4	2–3 M NaCl/KCl + 10 mM $MgCl_2$

1.2. Critical factors for ligand-RNA interaction evaluation by biosensor-SPR methods

1.2.1. RNase-free biacore T200 instrument

It is important for experiments with RNA to generate an RNase free environment. The instrument, glassware and the working area have to be treated with RNase*Zap* (Ambion, Austin, Texas) or a similar solution, to completely remove RNase contamination. To make the instrument RNase free, after GE recommended desorb and super clean, three times desorb with 50% (v/v) RNaseZap solution should be run followed by 12 h of manual run (25 µl/min) with DEPC treated autoclaved water (see below for details).

1. RNase-free water can be obtained commercially or from a Milli-Q® Water Purification System (MIlliporeSigma, Burlington, MA). In case double distilled water is used in the experiment, RNase removal can be achieved by incubating 0.1% (v/v) DEPC for 12 hrs at room temperature, followed by autoclaving for 40 min.
2. Glassware used in the experiment can be treated with Rnase Zap or similar solution then rinses with DEPC-treated water at least 2 times.
3. For SPR instrument cleaning, after the standard desorb procedure, follow by the standard super clean procedure an additional desorbs procedure with 50% (v/v) RNaseZap for 3 times was used to eliminate the possible presence of RNase residue in the fluidic system.
4. After the RNaseZap desorb procedure, the instrument is put on manual run with the flow rate 25 uL/min for 12 hrs or overnight with DEPC-treated water to remove any excess RNaseZap from the system.
5. We have found that this procedure allows preparation of RNA immobilized sensor chips that have excellent long-term stability, typically four weeks for average 25 individual experiments.

1.2.2. Concentration range and binding affinity K_D

For accurate determination of equilibrium constants by any method, the selected set of experimental concentrations must provide both free and bound concentrations of reactants. In the biosensor-SPR method with RNA immobilized to the surface, the ligand concentrations should be below and above K_D, ideally within 10-fold of the K_D, so that a range of bound fractions of ligand to RNA is obtained. The initial ligand concentrations have less binding to the RNA sites but as the concentration of ligand injected is increased, and the fraction of sites bound on RNA increases and approaches the saturation level. The sensorgrams have very low binding response reflected in RU at lower ligand concentrations and will approach saturation (RU change is small) with higher response at higher ligand concentrations. In this way, a series of sensorgrams with broad ligand concentrations will enable accurate determination of equilibrium constants. If the range of ligand concentrations used is too low or too high, accurate estimation of reaction rates and binding constants is not possible. Some preliminary testing is recommended when the ligand-target approximate K_D is unknown in order to establish an appropriate range of working ligand concentration.

1.2.3. Mass transport in association and rebinding in dissociation

For the ligand to bind to the RNA (or any target) immobilized to the sensor surface, the reactant in the solution injected over the flow cell surface must be transported from the bulk solution to the immobilized target surface, a phenomenon known as mass transport. This is a diffusion-controlled process, and the transport rate can directly influence the binding kinetics, if the rate occurs slower than the binding reaction. A key requirement for accurate determination of kinetic constants by the SPR method is that the amount of free ligand in the matrix must quickly equilibrate with the flow solution. The equilibration is assisted by using high flow rates (generally 100 µl/min in Biacore T200) to minimize reactant depletion. If the association reaction is much faster than mass transport, the observed binding will be limited by the mass transport process. Conversely, if the transport rate is faster than the association rate, the observed binding will represent the true interaction kinetics [36,39]. Therefore, mass transport is a critical factor that must be considered in biosensor experimental design and in evaluating kinetic constants from biosensor-SPR methods.

Overall, for kinetic measurements, it is generally recommended to use low surface densities of the immobilized RNA and high ligand flow rate to minimize the limitations on binding rates by mass transport processes. The optimal immobilized RU for a kinetic study is between 50 and 100 RU_{max} at the saturation level [40] for most small molecules. If the rate constants do not change at different flow rates, it indicates that true reaction kinetics are being obtained [39]. In addition, the dissociation phase can be set up for several hours or even longer with Biacore SPR, which allows at least 50% of bound ligand to dissociate, and a reliable kinetic fit can be performed, even with very slow dissociation.

2. Materials

2.1. Instrumentation

Biacore instruments use real-time label-free biomolecular interaction surface with surface plasmon resonance detection technology. A four channel Biacore instrument, the Biacore T200 (GE Healthcare Inc.), is currently the most sensitive research instrument and is useful for most research studies (note that many other sensitive instruments are being developed and comparisons can be done before purchase). Biacore T200 instruments use sensor chips with four channels such that, for example, three RNAs can be immobilized with one flow cell left blank as a control for bulk refractive index subtraction. With a sensor surface that has covalently attached streptavidin, a nucleic acid strand with biotin linked to either the 5′ or 3′ terminus can be easily captured to create the bio-specific surface. The specifications of the instrument are given on the GE Biacore web site https://www.biacore.com/lifesciences/index.html. The materials and procedures presented here are generally for Biacore instrumentation, but similar reagents and methods are used in other instruments.

2.1.1. Required materials for biacore general instrument cleaning and checking

1. RNAse free water such as diethyl pyrocarbonate (DEPC) treated autoclaved water. (0.01% (v/v) DEPC treated ddH_2O for at least 12 hrs then autoclaved for 40 min to inactivate DEPC since it is harmful to RNA.
2. A maintenance chip with a glass flow cell surface (available from GE Healthcare Inc,).
3. Desorb solution 1 and 2 (purchased from GE Healthcare or can be prepared)
   1%2 0.5% sodium dodecyl sulfate (SDS, Biacore desorb solution 1).
   2%2 50 mM glycine pH 9.5 (Biacore desorb solution 2) (*see* Note 2).
4. Super Clean solution (user prepared):
   a. 1% (v/v) acetic acid solution.
   b. 0.2 M sodium bicarbonate solution.
   c. 6 M guanidine hydrochloride solution.
   d. 10 mM HCl solution (see Note 3).
5. HBS–N buffer: 10 mM HEPES pH 7.4, 150 mM NaCl (user prepared or available from GE Healthcare Inc.) as a running buffer for system check.
6. BiaTest Solution: 15% (w/w) sucrose in HBS-EP buffer as an injecting buffer during system check (user prepared or available from GE Healthcare Inc.
7. 50% (v/v) RNaseZ™ as desorb solution (for experiments with RNA but not required for DNA or proteins).

2.2. Required materials for RNA immobilization on a sensor chip surface

1. CM5 sensor chip that has been at room temperature for at least 30 min prior to use (sensor chips are available from GE Healthcare Inc, *see* Note 1).
2. HBS–EP buffer: 10 mM HEPES pH 7.4, 150 mM NaCl, 3 mM EDTA, 0.05% v/v polysorbate 20 (user prepared or available from GE Healthcare Inc.) (Running buffer should be made in DEPC-treated autoclaved ddH_2O).
3. Thoroughly filter and degas all solutions for at least 20 mins. It should be emphasized that the internal microfluidics flow system of the instrument can be damaged by particulate matter present in any solution.
4. 100 mM N-hydroxysuccinimide (NHS) freshly prepared in DEPC-treated autoclaved ddH_2O.
5. 400 mM N-ethyl-N′-(dimethylaminopropyl) carbodiimide (EDC) freshly prepared in DEPC-treated autoclaved ddH_2O.
6. mM acetate buffer pH 4.5 (immobilization buffer).
7. 200–400 mg/ml streptavidin prepared in immobilization buffer.
8. M ethanolamine hydrochloride in water pH 8.5 (deactivation solution).
9. Activation buffer (1 M NaCl, 50 mM NaOH).
10. Biotin-labeled nucleic acid solutions (~25 nM of a single strand of hairpin RNA dissolved in HBS-EP buffer).

2.3. Sensor chip preparation for RNA immobilization

2.3.1. Preparation of streptavidin surface on CM5 chip

1. Dock the CM5 chip and prime with running buffer (*see* Note 1). A manual run is used to establish a stable baseline (the difference in RU over a period of time (ΔRU) < 1 for at least 60 sec) with a flow rate of 5 µl/min which is required to best make a streptavidin functionalized chip. “Dock” and “Prime” are Biacore software commands that instruct the instrument to carry out specific operations. The commands and operations are listed in Table 2.
2. A solution mixture comprised equal part of 100 mM NHS and 400 mM EDC is used. We recommend at least 75 µl of freshly prepared NHS and 75 µl of 400 mM EDC is required to activate the carboxymethyl surface to reactive esters (Fig. 2A). Note: mix these solutions just prior to injection to get good activation of the surface.
3. Manually inject the NHS/EDC mixture with the “Manual Inject” command in the Manual run for at least 10 min (50 µl) to receive the optimum amount of reactive esters, where ΔRU between before and after the mixture injection is around 150–200 RU for CM5 sensor chip. Repeat the above if necessary, to achieve the desired level of reactive esters for RNA experimental conditions.
4. By using “Manual Inject” command with a flow rate of 5 µl/min several injections of streptavidin, prepared in immobilization buffer, are injected over all four flow cells (Fig. 2A). The number of RUs immobilized (the difference between before and after streptavidin injection), which is available in real time readout are tracked to obtain the desired RU level. This is typically 2500–3000 RUs for a CM5 chip after the injection has been stopped. Repeat if necessary, to achieve the desired level of streptavidin.
5. For the deactivation of any remaining ester, 1 M ethanolamine hydrochloride with a flow rate of 5 µl/min, for 10 min is injected in all flow cells. Manually track the ΔRU before and after the ethanolamine injection, it should fall in between 20 and 25 RU.
6. At least five prime commends (Table 2) are necessary to obtain a stable baseline after deactivating the remaining ester.

2.3.2. Preparation of RNA

As examples, we have used 5′-Biotinylated RNA of $r(CUG)_5$, $r(GC)_4$ and TERRA (Fig. 1B) which can be obtained directly from several companies such as, Integrated DNA Technologies (IDT) and Dharmacon. RNA pellets are spun down in the tubes and 200 µl of HBS-EP buffer and for TERRA 25 mM Na_2HPO_4-NaH_2PO_4, pH = 7.2, 50 mM KCl, 1 mM EDTA buffer (note that, all buffers are prepared in DEPC treated autoclaved water) are added to each tube of RNA (~0.5 mM). After the pellets have been completely dissolved by pipetting up and down, vortex the tubes for 10 s and spin down for 10 s. 10 aliquots (each has 20 µl) of each RNA sequence are prepared in thermocycler tubes. The triplet repeats RNA sequence, $r(CUG)_5$ and $r(GC)_4$ are renatured by heating to 80 °C for 2 min and slowly cooling to room temperature by using RNaseZap-treated surface thermocycler. The G-quadruplex TERRA sequence is annealed by heating at 90 °C for 5 min and slowly cooling to room temperature in the thermocycler.

2.3.3. RNA immobilization on a streptavidin chip

1. A streptavidin-coated sensor chip that has been at room temperature for at least 30 min is required.
2. Biotin-labeled renatured RNA solution (~25 nM RNA dissolved in HBS-EP buffer (running buffer)) is required.
3. Dock the streptavidin-coated chip and by using the command manual run (Table 2). A sensorgram with a 25 µl/min flow rate is started to establish a stable base line with ΔRU < 1 for at least 60 sec.
4. Activation buffer, 1 M NaCl, 50 mM NaOH, is injected for 3 min (75 µl) for a course of five to seven times to remove unbound streptavidin from the sensor chip. The ΔRU of the base line for the last two consecutive cycles should be around 20–25.
5. To ensure the surface stability, prime with running buffer a few times (recommended minimum five times) is necessary.
6. Allow buffer to flow at least 20 min (or until the baseline is stable) before immobilizing the nucleic acids. It is important to have excess buffer flow through the fluidic system to ensure the system is free of NaOH, since strong base can damage RNA.
7. A new sensorgram with a flow rate of 1 µl/min is started in the desired flow cell under “flow path” (e.g., flow cell 2, fc2) to immobilize the nucleic acid. Generally, flow cell 1 (fc1) is used as a control and is left blank (i.e., without any immobilized RNA) for subtraction. It is often desirable to immobilize different nucleic acids on the remaining two flow cells (fc3 and fc4).
8. Establish a stable baseline within the manual run cycle with at least 120 sec wait time increment. Wait for the baseline to stabilize (which usually takes a few minutes), use “Manual Inject” to load the injection loop with ~100 µl of a 25 nM biotinylated nucleic acid solution for injection over the selected flow cell. Track the amount of RUs immobilized and stop the injection after the desired level is reached (typically ~200 RU for 20–30 base-pair RNA for kinetics experiments to minimize mass transport effects). If only an equilibrium constant is needed and not kinetics, higher RU can be immobilized.
9. At the end of the injection and after the baseline is stabilized, determine the RUs of the immobilized nucleic acid by using the reference line option and trace the ΔRU before and after the injection (Fig. 3). The amount of RNA immobilized is required to determine the theoretical moles of ligand binding sites for the current flow cell (*see* Note 4, Eq. (6)).
10. Repeat the steps 8 and 9 for immobilization of other RNAs to flow cells fc3 and fc4 separately.
11. After successful RNAs immobilization in all cells (Fig. 3, fc3, $r(CUG)_5$ immobilization, as an example) (except fc1) immobilization buffer is replaced by the experimental buffer. The system “prime commends” (Table 2) is then used several times.

2.4. Flow Solutions: Buffers and samples

2.4.1. General Buffers: (see Note 5)

The following buffers in DEPC treated autoclaved ddH_2O are

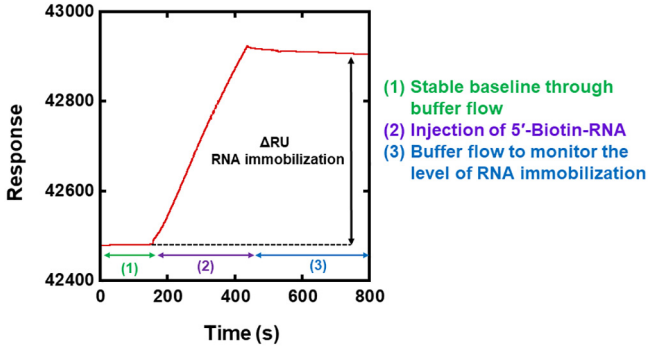

Fig. 3. Example for immobilization of biotin-labeled RNA on a streptavidin chip. The triplet repeats RNA, r(CUG)$_5$, is immobilized in flow cell 3 (fc3).

needed:

(1) (i) 10 mM HEPES pH 7.4, 150 mM NaCl, 3 mM EDTA, 0.05% 1X surfactant Tween 20. (HBS–EP buffer) (GE Healthcare Inc.) (see Note 6).

(ii) 25 mM Na_2HPO_4, PH 7.4, 150 mM KCl, 1 mM EDTA, 0.05% 1X surfactant Tween 20. Other KCl concentration can also be used.

(iii) 10 mM MES [2-(N-morpholino) ethanesulfonic acid] pH 6.25, 100 mM NaCl, 1 mM EDTA, and 0.05% 1X surfactant Tween 20. (MES10 buffer).

(iv) 10 mM CCL [cacodylic acid] pH 6.25, 100 mM NaCl, 1 mM EDTA, and 0.05% surfactant 1X surfactant Tween 20. (CCL10 buffer).

(v)10 mM Tris [(hydroxymethyl) aminomethane] pH 7.4, 100 mM NaCl, 1 mM EDTA, and 1X surfactant Tween 20, (Tris10 buffer).

2. The sample solution must be prepared in the same buffer used to establish the baseline (running buffer) (*see* Note 7).
3. As described above, the sample concentration to be used depends on the magnitude of the equilibrium dissociation constant (K_D). A large concentration range above and below K_D will yield a reliable/accurate binding curve. For binding constants of 10^7–10^8 M^{-1}, as observed with many nucleic acid/small molecule complexes, small molecule concentrations from about 1 nM to 10 μM in the flow solution allow accurate determination of binding constants. Injecting samples from low to high concentration is useful as it prevents data artifacts from ligand adsorption. For nM and lower K_D, the lower concentration must be used (*see* Note 8).
4. Possible problems at high sample concentrations: poor sensorgrams, non–specific binding, ligand aggregation may be obtained. In this case, only the lower concentrations can be used for quantification.

2.4.2. Regeneration solution (see Note 9)

1. Appropriate regeneration conditions help achieve complete removal of the bound ligand from the chip surface without degrading the immobilized target. Commonly used regeneration solutions are listed in Table 3. In general, milder conditions are recommended for initial use, while more stringent conditions are applied only as needed. Regeneration solutions for different samples are available in the Biacore website https://www.biacore.com/lifesciences/index.html. In our RNA-organic small molecules interactions studies, 1 M KCl is typically used as an efficient regeneration agent to remove small molecules from the RNA immobilized sensor chip surface while keeping the RNA folded structure intact on the sensor chip.
2. Inject 100 μl of regeneration solution at high 100 μl/min flow rates to assure efficient regeneration.
3. After injection of the regeneration solution, three cycles of 1-min injections of running buffer are recommended to wash off the remaining regeneration solution.
4. At the end of each cycle, a 5 min running buffer flow is also recommended to ensure that the chip surface is re-equilibrated for binding (i.e., the dextran matrix is re-equilibrated with running buffer) and that the baseline is stabilized before the following sample injection.

2.5. Possible immobilization and amine coupling

There are several ways of immobilizing substances to the sensor surface. The choice of immobilization methods depends on the properties of the substance. The immobilization approaches may be directed towards amine, carboxyl, thiol or hydroxyl groups on the ligand, or may use specific tags introduced into the ligand (Table 1).

2.5.1. Amine coupling

Amine coupling chemistry is another widely applicable approach for covalently attaching biomolecules to the sensor chip surface and is suitable for the ligand included in the Getting Started Kit. With this method, the dextran matrix on the sensor chip surface is first activated with a mixture of 1-ethyl-3- (3-dimethylaminopropyl) carbodiimide (EDC) and N-hydroxysuccinimide (NHS) to give reactive succinimide esters. Ligand is then passed over the surface, and the esters react spontaneously with amino groups or other nucleophilic groups to link the ligand covalently to the dextran. After the injection of ligand, ethanolamine is passed over the sensor surface to deactivate remaining active esters (Fig. 2A).

3. Method

The Biacore software, supplied with the instrument, allows users to write a method or to use a software wizard to set up experiments. Several important factors, such as flow rate, association and dissociation times, injection order and surface regeneration must be considered while setting up an experiment. A simple method used to collect small molecule binding results on RNA surfaces is shown below. The compounds (DB 1246, DB75, and DB182, prepared in the laboratory of Professor D. W. Boykin at GSU, and Neomycin is commercially available) and the biotin-labeled RNA sequences (r(CUG)$_5$, r(GC)$_4$, TERRA) used in this experiment are shown in Fig. 1.

3.1. Data collection and processing

1. A four-channel Biacore instrument, typically a T200 (GE Healthcare Inc.), is advantageous for small molecule binding to RNA. This instrument was used in the experiments described in this review.
5. Three different 5′-biotin-labeled RNAs can be immobilized, each one immobilized in a distinct flow cell of a SA chip, as described in 2.3.1. Approximately the same moles of each RNA oligomer are immobilized on the surface of these flow cells to compare the sensorgram saturation levels directly for stoichiometry determination.
6. An appropriate regeneration solution is selected for the complex formed in the experiment. Relatively weak binders frequently dissociate on their own. Somewhat stronger binders can be dissociated with a 1 M NaCl or KCl solution while still stronger binders require a more drastic treatment (see Table 3 for other regeneration buffers).
7. Serial dilutions (concentration range, for example, from 5 nM to 10 μM) of the binding compound are prepared using the running buffer as the diluent to minimize changes in the refractive index caused by buffer components. The flow rate is set to 100 μl/min where possible to minimize mass transport (*see* Note 10).
8. Five buffer samples are typically injected at the beginning of each experiment to evaluate if the instrument is performing within specifications and establish a baseline for subtraction. This is a method called double referencing. (see Note 14) [41].

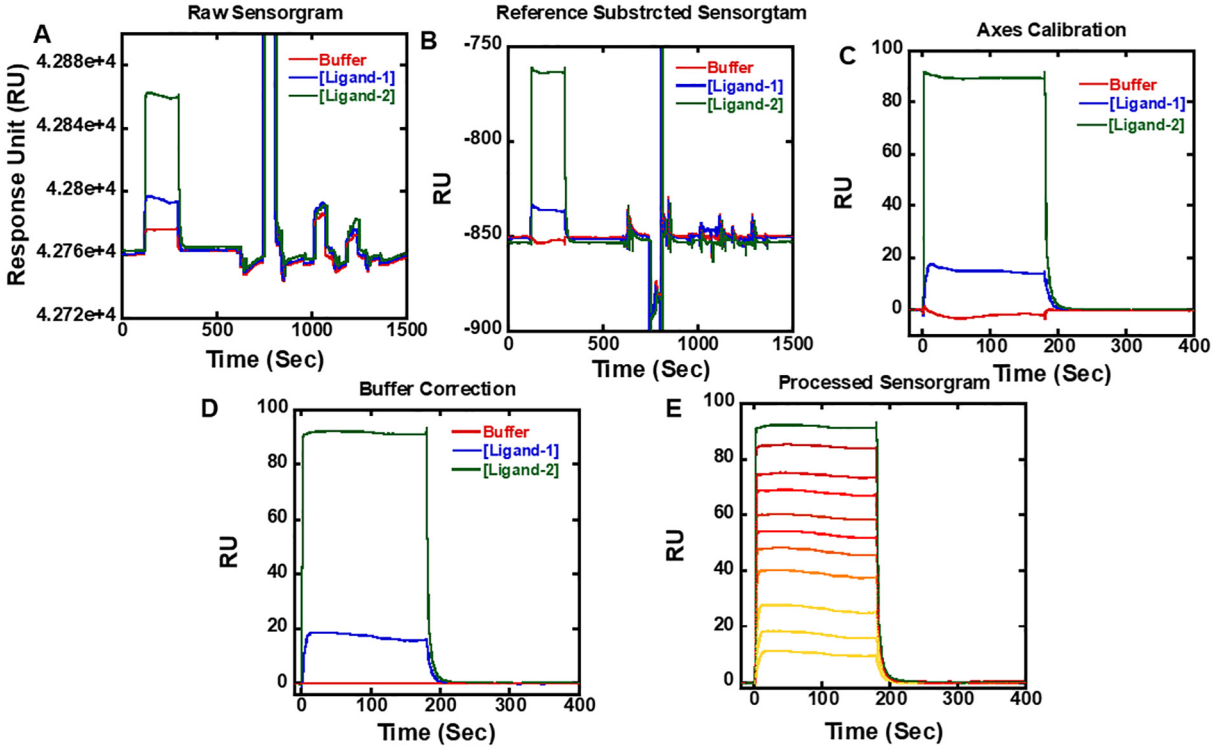

Fig. 4. Processing biosensor data. (A) Raw data from biosensor for DB182 injected over the r(CUG)$_5$ RNA sequence or surface; (B) Data sets from the reference surface were subtracted from the data from the reaction surface; (C) Axes calibration data obtained from Biaevaluation software by using kinetic/affinity commands; (D) Corrections of the response from the blank buffer injections; (E) Overlay of a series of DB182 injections.

Buffer injections also serve as controls for data processing.

9. Inject 300 µl (3 min) of each compound concentration and set 600 s (these are varied with different compounds and kinetics) as dissociation time (*see* Note 11). Inject samples from low to high concentration to eliminate data artifacts from ligand carryover or contamination of the instrument flow system (*see* Note 12). Random injection of concentrations can also use to minimize data artifact.
10. At the end of the dissociation phase, inject one short pulse (typically 30 – 60 s) of regeneration buffer, such as, 1 M KCl followed by three 1-min injections of running buffers are recommended to reduce the remaining regeneration solution and 5 min running with buffer flowing is also set to ensure that the chip surface is re-equilibrated for binding (*see* subheading 2.4.2. step 3).
11. When the experiment is completed, open the raw data containing the sensorgrams in the Biaevaluation software for data processing software or Scrubber 2 or other (*see* Note 13, Fig. 4). First, zero the sensorgrams on the y-axis (RU) to allow proper comparison of the responses of each flow cell. Generally, the average of a stable time region of the sensorgram, prior to sample injection, should be selected and set to zero for each sensorgram. Then, zero on the x-axis (time) to align the beginnings of the injections with respect to each other [41].
12. Subtract the control flow cell (fc1) sensorgram from the reaction flow cell sensorgrams (i.e. fc2–fc1, fc3–fc1, and fc4–fc1). This removes any bulk shift contribution to the change in RUs (Fig. 4).
13. Subtract a buffer injection (the injection with a ligand concentration of zero), or better, an average of several buffer injections from the compound injections (different concentrations) on the same reaction flow cell (*see* Note 14). This is known as double subtraction and removes any flow cell specific baseline irregularities (Fig. 4) [41,42]. At this point, the data should be of optimum quality and ready for analysis as described below.
14. Sensorgrams after the previous step can be extracted to a text file and graphed in other graphics software such as KaleidaGraph (Synergy software).
15. Steady-state and kinetic data can be further extracted for quantitative analysis of the interaction via the tab “kinetic or affinity” (Table 2) provided in Biaevaluation software. These data can also be extracted into a text file and further analyze in third-party graphics software. Fig. 5 shows the representative steady-state point obtained from the sensorgrams, and Fig. 9

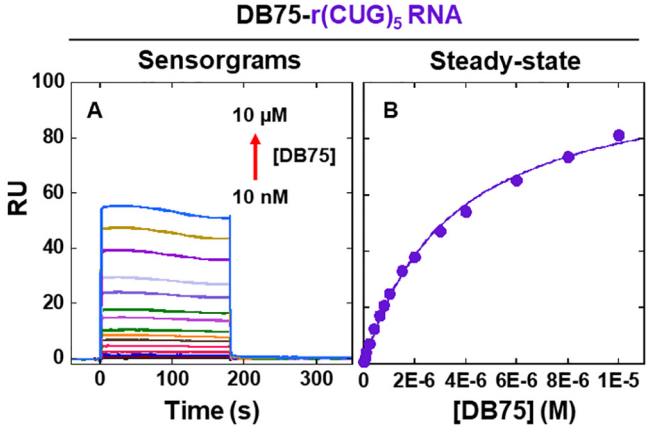

Fig. 5. DB75 interaction with r(CUG)$_5$ RNA sequence. (A) A representative set of sensorgrams with graded concentrations of DB75 are shown in the figure (red arrow) from 10 nM to 10 µM; (B) The corresponding RU at steady state is shown. Data were the best fit with an independent binding site size model (Eqs. (6) and (7)) with N = 8 ± 1, K_D = 3.4 ± 0.22 µM. (For interpretation of the references to colour in this figure legend, the reader is referred to the web version of this article.)

show the kinetic fit from the sensorgrams.

4. Examples of use of the SPR method with RNA

In this report, we have extended an SPR protocol that has been previously developed for working with DNA and small molecules. Our goal is to develop a quantitative assay using SPR as a primary technique to observe the interaction between small molecules with different RNA sequences. In this report, r(CUG)$_5$, r(GC)$_4$ and the quadruplex telomeric RNA sequence (TERRA) have been used as examples.

The triplet repeat r(CUG)$_5$ is directly associated with the neurological disorder myotonic dystrophy type 1 (DM1). That sequence has been used extensively as a model for drug development against DM1 [24,43] but has been rarely used with SPR. Fig. 5A shows representative sensorgrams of furamidine, DB75, binding to the r(CUG)$_5$ RNA sequence. The sensorgrams show fast dissociation and association kinetics for the molecules tested and RNA sequences. Under these conditions, there is no significant aggregation observed at high concentrations, up to 10 μM of DB75, Furamidine, and other diamidines (Fig. 1), due to the high solubility and excellent solution properties of the compounds. The equilibrium dissociation constant K_D is obtained through a steady-state fitting, where the RU signal is recorded at the steady state plateau for each sensorgram at different compound concentrations. Fig. 5B shows the result with the best curve fitting obtained by an independent, identical binding site for DB75 with RNA (Eqs. (7) and (8)). The K_D is 3.4 ± 0.22 μM corresponding to N = 8 ± 1 molecules bind to RNA. This result is in good agreement with the previous study where the Berglund group showed that furamidine binds to r(CUG)$_4$ with K_D of approximately 100 nM in a lower salt environment, 25 mM NaCl versus 150 mM KCl used in our experiment, and N = 6 ± 1 molecule [43]. It is worth mentioning that our SPR result is in good agreement with ITC results from the Berglund group. This is another validation of SPR as a reliable, label-free technique to quantitatively decipher the interactions of small molecules and RNA .

$$r = \frac{NKC_{free}}{1 + KC_{free}} \tag{7}$$

where:

$$r = \frac{RU_{obs}}{RU_{max}} \tag{8}$$

K is the equilibrium binding constant, C_{free} is the concentration of the compound, N is the number of molecules independently bind to the RNA sequence. RU_{obs} is the observed steady state RU from the experiment, RU_{max} is the calculated RU for single molecule bind to RNA. This can be obtained from Eq. (6).

Further, we have demonstrated the binding interactions of the tetracation DB182 (Fig. 1) with r(GC)$_4$ an RNA model duplex sequence. DB182 has been shown to be a promising molecule that inhibits HIV RRE-Rev interaction [15]. As shown in Fig. 6A, the sensorgrams indicate that the DB182 interactions with r(GC)$_4$ also have fast association and dissociation kinetics under our conditions. The K_D value obtained from steady state analysis has shown the best fit with K_D = 3.1 ± 0.22 μM and N = 4 ± 1 molecule. Since r(GC)$_4$ is a shorter sequence compared to r(CUG)$_5$ (8 bp versus 15 bp), it is understandable that r(GC)$_4$ has fewer available binding sites for DB182, assuming both DB182 and DB75 similarly interact with RNA.

We also investigated the interaction of diamidine compounds to a quadruplex, TERRA, a telomeric RNA sequence. DB1246 has been shown in previous studies to be a promising therapeutic molecule that targets G4C2 repeat quadruplex RNA sequence that causes toxicity [44]. The repeat expansion of G4C2 found in C9orf72 is the common cause for frontotemporal dementia and amyotrophic lateral sclerosis (ALS) neurodegenerative diseases [44]. Fig. 7A shows the sensorgrams for the interaction of DB1246 with TERRA up to 250 nM concentration of the compounds. DB1246 shows strong binding to the TERRA RNA

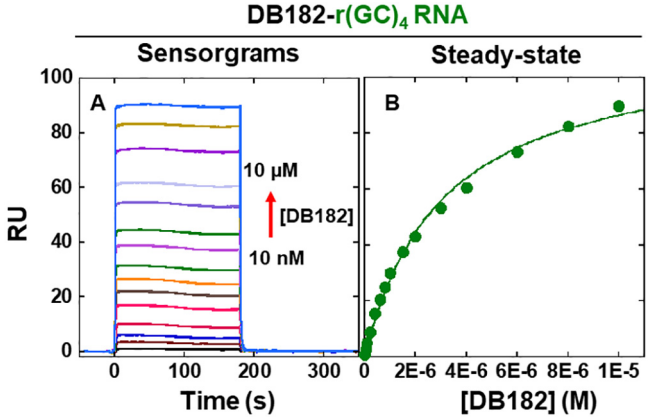

Fig. 6. DB182 interaction with the r(GC)$_4$ RNA sequence. (A) A representative set of sensorgrams with graded concentrations of DB182 are shown in the figure (red arrow) from 10 nM to 10 μM; (B) The corresponding RU at steady state, as in Fig. 5, data were best fit with an independent binding site size model (Eqs. (6) and (7)) with N = 4 ± 1, K_D = 3.1 ± 0.22 μM. (For interpretation of the references to colour in this figure legend, the reader is referred to the web version of this article.)

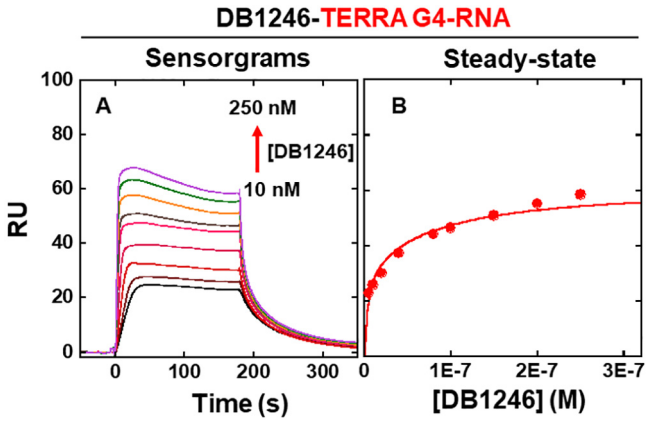

Fig. 7. DB1246 interaction with the TERRA G4-RNA sequence. (A) A representative set of sensorgrams with graded concentrations of DB1246 are shown in the figure (red arrow) from 10 nM to 250 nM; (B) The corresponding RU at steady state as in Fig. 5, data were best fit with two binding site model (Eq. (9)) with K_{D1} = 3 ± 0.8 nM and K_{D2} = 80 ± 12 nM. (For interpretation of the references to colour in this figure legend, the reader is referred to the web version of this article.)

model sequence, as expected for compounds specifically targeting quadruplex RNA. Kinetic interactions between DB1246 and TERRA are identified by fast association and slower dissociation (90% dissociation in 100 sec compared with > 95% dissociation in < 20 sec for the interaction of DB75 and DB182 with other RNAs) kinetics. The steady-state result shows a two-site binding model (Eq. (9)) that is fit best to yield binding constants K_{D1} = 3 ± 0.8 nM and K_{D2} = 80 ± 12 nM. This is one of the strongest quadruplex RNA binders in the heterocyclic diamidine group of small molecules. The equation for a two-site model is shown below:

$$r = \frac{K_1 C_{free} + 2K_1 K_2 C_{free}^2}{1 + K_1 C_{free} + K_1 K_2 C_{free}^2} \tag{9}$$

where K_1 and K_2 are the macroscopic equilibrium binding constants, and C_{free} is the concentration of the free compound.

We also analyzed the interaction of neomycin to the RNA sequences. Fig. 8 show the steady-state result for interactions of neomycin to r(GC)$_4$, r(CUG)$_5$ and TERRA sequences. The data were also fitted with Eq. (7) for multiple independent binding site. The steady-state result

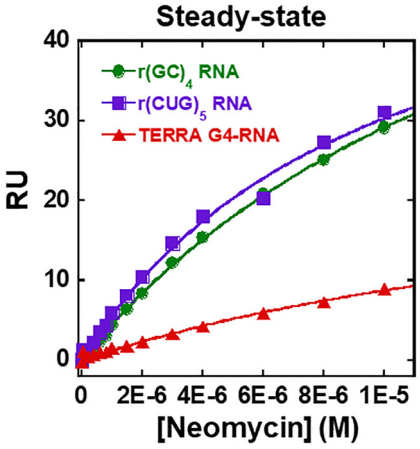

Fig. 8. Steady state result of Neomycin interaction with all 3 RNA sequences: with $r(GC)_4$ RNA (●), with $r(CUG)_5$ RNA (■) and with TERRA G4-RNA (▲). Data were fitted with independent, identical binding site for $r(GC)_4$ DNA $K_D = 16.2 \pm 0.11\,\mu M$, $N = 2 \pm 1$; $r(CUG)_5$ RNA $K_D = 9.6 \pm 1.2\,\mu M$, $N = 3 \pm 1$; TERRA G4-DNA model $K_D = 22 \pm 7.2\,\mu M$, $N = 1 \pm 1$.

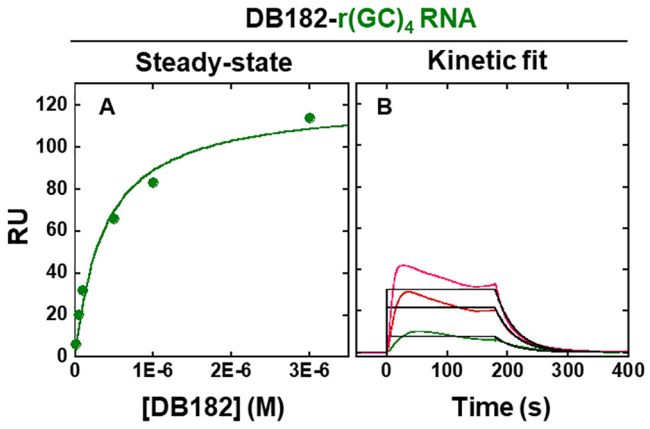

Fig. 9. DB182 interaction with the $r(GC)_4$ RNA sequence. (A) A steady state fit to obtain the K_D at 25 mM KCl. Steady state data were best fit with an independent binding site size model (Eqs. (6) and (7)) with $K_D = 0.37 \pm 0.09\,\mu M$, $N = 6 \pm 1$; (B) Representative sensorgrams with graded concentrations of DB182: 10, 50 and 100 nM (colored) and dissociation kinetic fitting curve (black), $k_d = 0.03 \pm 0.002\,s^{-1}$, k_a average (estimated) = $(8.11 \pm 2.04) \times 10^4\ M^{-1}s^{-1}$.

show that neomycin bound to both $r(GC)_4$ and $r(CUG)_5$ with similar affinities, $K_D = 16.2 \pm 0.11\,\mu M$, $N = 2 \pm 1$ molecules for $r(GC)_4$ and $K_D = 9.6 \pm 1.2\,\mu M$, $N = 3 \pm 1$ molecules. Since the size of neomycin is larger than that of heterocyclic amidines compounds, it is to expect there were fewer molecules that bound to the RNA sequences. Neomycin exhibited poor interaction with TERRA G4 RNA sequence with the $K_D = 22 \pm 7.2\,\mu M$, $N = 1 \pm 1$ molecules. This is > 250-fold weaker than the binding affinities of DB1246 to TERRA.

These results demonstrate the ability of biosensor-SPR methods to measure the binding interactions of RNA and small molecules from a thermodynamic perspective. Another powerful SPR application is dissecting the kinetic rate constants of the interaction, therefore providing molecular details of the interaction mechanism. Fig. 9 shows the interaction of DB182 with $r(GC)_4$ RNA in a low salt condition (25 mM KCl). Fig. 9A shows the steady-state fit with the $K_D = 0.37 \pm 0.09\,\mu M$ and $N = 6 \pm 1$ molecules. It is logical that the molecules have a stronger binding affinity in a low salt condition (compare to $K_D = 3.2 \pm 0.09\,\mu M$ at 150 mM KCl). The number of the molecules associated with the RNA remained unchanged since it is the same RNA sequence. Fig. 9B showed dissociation kinetic rate curve fitting in black from the sensorgrams represented the interaction DB182 to $r(GC)_4$ RNA using Scrubber2 software (BioLogic Software, Campell, Australia). The sensorgrams at lower concentrations of DB182 from 10 to 100 nM show a drift in steady state in the early injections but reach a plateau near the end of the injection. This curvature in sensorgrams might reflect the strong ionic interaction between the tetracation compounds with the polyanion RNA sequence at the low salt condition, e.g., 25 mM KCl. Since there are approximately 6 DB182 molecules bind to $r(GC)_4$ RNA, the average association rate constant k_a was obtained using the known K_D and k_d values. The calculated k_a equal to $8.11 \times 10^4\ M^{-1}s^{-1}$, reflected the overall association rate of multiple, independent binding events of DB182 to $r(GC)_4$ RNA. Altogether, the data have shown that SPR is capable of dissecting thermodynamics and kinetic information from the interaction of small molecules with RNA. This will help to understand further the structure–function relationship and development of molecules that are in the therapeutic interest.

5. Concluding statement

In this review we have described the application of biosensor-SPR methods from the early studies and instruments to the present day. The currently available instruments are very sensitive, and new instruments are being released frequently. The power and attraction of the instruments are that they provide a label-free method that uses very little material to deliver interaction affinity, kinetics and stoichiometry for biomolecular complex formation. The SPR experiments can also be done as a function of temperature. It is certain that the use of this technology with RNA will expand in the future to help characterize existing systems as well as new RNAs and agents which bind to them. The use of SPR methods in the search for new therapeutic agents that target RNA should also expand well past the studies described in this chapter.

6. Notes

1. The choice of sensor chip depends on the nature and demands of the application. For general purposes, a Biacore CM5 sensor chip, which carries a hydrophilic matrix of carboxymethylated (CM) dextran covalently attached to the gold surface, can be used. It has a high surface capacity for immobilizing a wide range of ligands from protein to nucleic acids and carbohydrates. For protein-RNA interaction investigation, the Biacore CM4 sensor chip is another good choice because it is similar to sensor chip CM5 but has a lower degree of carboxymethylation (~30% of CM5 chip) and charge that helps to reduce non-specific binding of highly positively charged molecules, such as proteins, to the surface. Streptavidin-coated sensor chip has a surface carrying a dextran matrix to which streptavidin has been covalently attached. Streptavidin has a very high binding affinity for biotin ($K_D \approx 10^{-15}$ M) so that the surface provides a high capture of biotinylated ligands. The streptavidin-coated chip is particularly suited for nucleic acid immobilization since biotin coupling of oligonucleotides at the terminal, or the internal positions is a well-established procedure. For some other specialized applications, a range of other sensor chips surfaces and immobilization chemistries are also available (Table 1).
2. Maintenance chips are available from GE Healthcare Inc. “Desorb” is a Biacore software command that instructs the instrument to remove adsorbed ligands from the flow system. A detailed list of commands and operations are shown in Table 2. Make sure that the analysis and sample compartment temperatures are not below 20 °C, since SDS in Desorb solution 1 will precipitate at low temperature.
3. After running the regular Desorb for the additional extensive cleaning additional super clean method may be used.
4. The amount of RNA to immobilize on the sensor chip depends on the relative molecular weight of the target RNA and of the ligand

and on the sensitivity of the biosensor system. Since the SPR response is directly proportional to the mass concentration of material on the surface, the theoretical ligand binding capacity for a 1:1 interaction of a given surface is relative to the amount of RNA immobilized.

5. The selection of experimental buffer depends on the nature of the ligand and RNA sequence. Salt concentration can be adjusted based on the experimental requirement. With the increase of ionic strength/salt concentration, the binding affinity of positively charged ligands for the negatively charged nucleic acid typically decreases due to charge shielding effects.
6. The amount of P20 to be used depends on the system, the instrument, and the sensor chip, typical concentrations between 0.05% and 0.005% are used. In a Biacore T200 instrument generally use 0.05%.
7. If the ligand requires the presence of a small amount of organic solvent (e.g., < 5% DMSO) to maintain solubility, a solvent correction needs to be applied to minimize changes in the refractive index caused by the organic content at the chip surface. This has been described in detail by Rich and Myszka [45].
8. If the K_D is unknown, it is necessary to conduct a preliminary experiment using a wide range of compound concentration to obtain an estimate of the K_D. A more focused set of concentrations is then prepared to cover the specific binding range.
9. Regeneration conditions must be harsh enough to break the complex and remove the bound ligand but mild enough to keep the RNA strand intact. It is highly recommended to start with the mildest conditions and short surface contact times since regeneration solutions can cause an undesired effect on RNA or immobilized matrix. A short contact time, 30–60 s, is usually sufficient. Longer exposure to regeneration conditions involves greater risks of loss of binding activity on the surface and often does not lead to improved regeneration.
10. For the steady-state method, equilibrium constants can be obtained but not kinetics constants even when mass transfer effects dominate the observed kinetics. Thus, higher flow rates are not required in steady-state experiments, if a clear steady–state plateau is obtained, to determine RU. Higher flow rates (> 50 µl/min) are used for kinetic experiments to minimize mass transport effects.
11. A sufficient association phase with a plateau region is needed for steady-state analysis. For the most accurate fitting of the dissociation phase, it is good practice to allow sufficient time for the compound to achieve at least 50–80% dissociation from the complex.
12. Many organic small molecules are easily adsorbed nonspecifically to the tubing of the injection microfluidics and are slowly released over the course of the experiment. Increasing surfactant concentration might reduce adsorbing to the tubing. If increasing concentrations of the binding sample in a series of injections are used, the nonspecific absorption problem can be elevated.
13. Other software programs such as Scrubber 2, CLAMP and GeneData are available for processing Biacore data. The results can also be exported and presented in graphing software such as KaleidaGraph. Although it is useful to experiment with different software packages, Biaevaluation is sufficient for most routine analyses of sensorgram data. For the Biacore T200 user, data processing can be performed automatically using the Biacore T200 evaluation software, which is convenient for new users. For the processing of Biacore data for large libraries of small molecules, GeneData is a preferred choice.
14. These two data processing steps are referred to as “double referencing.” Typically, multiple buffer injections are performed and averaged before subtraction. In double referencing, plots are made for each flow cell separately overlaying the control flow cell– corrected sensorgrams from the buffer and all sample injections. The buffer sensorgram is then subtracted from the sample sensorgrams. “Double referencing” removes the systematic drifts and shifts in baseline and is helpful to minimize offset artifacts and also to correct the bulk shift that results from slight differences in injection buffer and running buffer (see Fig. 4).
15. In some cases, at lower concentrations, where the response does not reach the steady-state, the equilibrium responses can be obtained from kinetic fits of the sensorgrams utilizing the known RUmax from the higher concentration sensorgrams. This extrapolation method works well with sensorgrams where the observed response is at least 50% of the equilibrium RU.

Acknowledgment

T.V. is supported by the Molecular Basis of Disease (MBD) fellowship from the College of Arts and Sciences, Georgia State University.

Funding

This work was supported by the US National Institutes of Health (NIH) [Grant No. GM111749 to W.D.W and D.W.B].

Conflicts of interest

The authors declare no conflict of interest.

References

[1] L.G. Fägerstam, A. Frostell-Karlsson, R. Karlsson, B. Persson, I. Rönnberg, Biospecific interaction analysis using surface plasmon resonance detection applied to kinetic, binding site and concentration analysis, J. Chromatogr. 597 (1–2) (1992) 397–410.
[2] I.D. Parsons, B. Persson, A. Mekhalfia, G.M. Blackburn, P.G. Stockley, Probing the molecular mechanism of action of co-repressor in the E. coli methionine repressor-operator complex using surface plasmon resonance (SPR), Nucleic Acids Res. 23 (2) (1995) 211–216.
[3] P.J. Bates, H.S. Dosanjh, S. Kumar, T.C. Jenkins, C.A. Laughton, S. Neidle, Detection and kinetic studies of triplex formation by oligodeoxynucleotides using real-time biomolecular interaction analysis (BIA), Nucleic Acids Res. 23 (18) (1995) 3627–3632.
[4] M.L. West, T.E. Ramsdale, Binding kinetics and bioassay of RRE mRNA fragments to a peptide containing the recognition domain of HIV-1 Rev, Biomed. Pept. Proteins Nucleic Acids 2 (3) (1996) 85–88.
[5] S. Park, D.G. Myszka, M. Yu, S.J. Littler, I.A. Laird-Offringa, HuD RNA recognition motifs play distinct roles in the formation of a stable complex with AU-rich RNA, Mol. Cell. Biol. 20 (13) (2000) 4765–4772.
[6] S.P. Ohuchi, Y. Nakamura, Slight sequence modifications unexpectedly alter the metal-dependency of a kissing-loop interaction, Nucleic Acids Symp. Ser. (Oxf) 51 (2007) 395–396.
[7] C.H. Wong, F.S. Liang, Surface plasmon resonance study of RNA-aminoglycoside interactions, Methods Enzymol. 362 (2003) 340–353.
[8] M. Hendrix, E.S. Priestley, G.F. Joyce, C.H. Wong, Direct observation of aminoglycoside−RNA interactions by surface plasmon resonance, J. Am. Chem. Soc. 119 (1997) 3641–3648.
[9] C.H. Wong, M. Hendrix, E.S. Priestley, W.A. Greenberg, Specificity of aminoglycoside antibiotics for the A-site of the decoding region of ribosomal RNA, Chem. Biol. 5 (1998) 397–406.
[10] A. Ironmonger, B. Whittaker, A.J. Baron, B. Clique, C.J. Adams, A.E. Ashcroft, P.G. Stockley, A. Nelson, Scanning conformational space with a library of stereo- and regiochemically diverse aminoglycoside derivatives: the discovery of new ligands for RNA hairpin sequences, Org. Biomol. Chem. 5 (7) (2007) 1081–1086.
[11] B. Davis, M. Afshar, G. Varani, A.I. Murchie, J. Karn, G. Lentzen, M. Drysdale, J. Bower, A.J. Potter, I.D. Starkey, T. Swarbrick, F. Aboul-ela, Rational design of inhibitors of HIV-1 TAR RNA through the stabilization of electrostatic “hot spots”, J. Mol. Biol. 336 (2004) 343–356.
[12] W. Tan, J. Zhou, J. Gu, M. Xu, X. Xu, G. Yuan, Probing the G-quadruplex from hsa-miR-3620-5p and inhibition of its interaction with the target sequence, Talanta 154 (2016) 560–566.
[13] W.D. Wilson, F.A. Tanious, A. Mathis, T.M. Davis, J.E. Hall, D.W. Boykin, Antiparasitic compounds that target DNA, Biochimie 90 (7) (2008) 999–1014.
[14] K. Li, T.M. Davis, C. Bailly, A. Kumar, D.W. Boykin, W.D. Wilson, A heterocyclic inhibitor of the Rev−RRE complex binds to RRE as a dimer, Biochemistry 40 (5) (2001) 1150–1158.
[15] G. Xiao, A. Kumar, K. Li, C.T. Rigl, M. Bajic, T.M. Davis, D.W. Boykin, W.D. Wilson, Inhibition of the HIV-1 Rev–RRE complex formation by unfused aromatic cations, Bioorganic Med. Chem. 9 (5) (2001) 1097–1113.
[16] N.W. Luedtke, Y. Tor, A novel solid-phase assembly for identifying potent and selective RNA ligands, Angew. Chem. Int. Ed. Engl. 39 (10) (2000) 1788–1790.

[17] K. Nakatani, S. Horie, Y. Goto, A. Kobori, S. Hagihara, Evaluation of mismatch-binding ligands as inhibitors for Rev-RRE interaction, Bioorg. Med. Chem. 14 (15) (2006) 5384–14388.

[18] L.A. Macfarlane, P.R. Murphy, MicroRNA: biogenesis, function and role in cancer, Curr. Genom. 11 (7) (2010) 537–561.

[19] M.F. Schmidt, Drug target miRNAs: chances and challenges, Trends Biotechnol. 32 (11) (2014) 578–585.

[20] T. Fukuzumi, A. Murata, H. Aikawa, Y. Harada, K. Nakatani, Exploratory study on the RNA-binding structural motifs by library screening targeting pre-miRNA-29 a, Chem. Eur. J. 21 (47) (2015) 16859–16867.

[21] J. Li, M. Nakamori, J. Matsumoto, A. Murata, C. Dohno, A. Kiliszek, K. Taylor, K. Sobczak, K. Nakatani, A dimeric 2,9-diamino-1,10-phenanthroline derivative improves alternative splicing in myotonic dystrophy type 1 cell and mouse models, Chem. Eur. J. 24 (68) (2018) 18115–18122.

[22] J. Li, J. Matsumoto, L.P. Bai, A. Murata, C. Dohno, K. Nakatani, A ligand that targets CUG trinucleotide repeats, Chem. Eur. J. 22 (42) (2016) 14881–14889.

[23] S.G. Rzuczek, L.A. Colgan, Y. Nakai, M.D. Cameron, D. Furling, R. Yasuda, M.D. Disney, Precise small-molecule recognition of a toxic CUG RNA repeat expansion, Nat. Chem. Biol. 13 (2) (2017) 188–193.

[24] L. Nguyen, L.M. Luu, S. Peng, J.F. Serrano, H.Y. Chan, S.C. Zimmerman, Rationally designed small molecules that target both the DNA and RNA causing myotonic dystrophy type 1, J. Am. Chem. Soc. 137 (44) (2015) 14180–14189.

[25] A. Iguchi, N. Fukuda, T. Takahashi, T. Watanabe, H. Matsuda, H. Nagase, T. Bando, H. Sugiyama, K. Shimizu, RNA binding properties of novel gene silencing pyrrole-imidazole polyamides, Biol. Pharm. Bull. 36 (7) (2013) 1152–1158.

[26] A. Donlic, A.E. Hargrove, Targeting RNA in mammalian systems with small molecules, Wiley Interdiscip. Rev. RNA. 9 (4) (2018) e1477.

[27] C.M. Connelly, M.H. Moon, J.S. Jr, Schneekloth, The emerging role of RNA as a therapeutic target for small molecules, Cell Chem. Biol. 23 (9) (2016) 1077–1090.

[28] M.D. Disney, B.G. Dwyer, J.L. Childs-Disney, Drugging the RNA world, Cold Spring Harb. Perspect. Biol. 10 (11) (2018) 1–15.

[29] K.D. Warner, C.E. Hajdin, K.M. Weeks, Principles for targeting RNA with drug-like small molecules, Nat. Rev. Drug Discov. 17 (8) (2018) 547–558.

[30] H. Sipova, J. Homola, Surface plasmon resonance sensing of nucleic acids: a review, Anal. Chim. Acta 773 (2013) 9–23.

[31] H.P. Ho, F.C. Loo, S.Y. Wu, D. Gu, K.T. Yong, S.K. Kong, MicroRNA biosensing with two-dimensional surface plasmon resonance imaging, Methods Mol. Biol. 1571 (2017) 117–127.

[32] H.H. Nguyen, J. Park, S. Kang, M. Kim, Surface plasmon resonance: a versatile technique for biosensor applications, Sensors (Basel) 15 (5) (2015) 10481–10510.

[33] C. Di Primo, E. Dausse, J.J. Toulme, Surface plasmon resonance investigation of RNA aptamer-RNA ligand interactions, Methods Mol. Biol. 764 (2011) 279–300.

[34] P.S. Katsamba, S. Park, I.A. Laird-Offringa, Kinetic studies of RNA-protein interactions using surface plasmon resonance, Methods 26 (2) (2002) 95–104.

[35] E. Coppari, S. Santini, A.R. Bizzarri, S. Cannistraro, Kinetics and binding geometries of the complex between β2-microglobulin and its antibody: an AFM and SPR study, Biophys. Chem. 211 (2016) 19–27.

[36] D.G. Myszka, Kinetic, equilibrium, and thermodynamic analysis of macromolecular interactions with BIACORE, Methods Enzymol. 323 (2000) 325–340.

[37] B. Nguyen, F.A. Tanious, W.D. Wilson, Biosensor-surface plasmon resonance: quantitative analysis of small molecule-nucleic acid interactions, Methods 42 (2007) 150–161.

[38] F.A. Tanious, B. Nguyen, W.D. Wilson, Biosensor-surface plasmon resonance methods for quantitative analysis of biomolecular interactions, in: J.J. Correia, H. W. Detrich, editors. Methods Cell Biol. 84. (2008) 53–77.

[39] R. Karlsson, Affinity analysis of non-steady-state data obtained under mass transport limited conditions using BIAcore technology, J. Mol. Recognit. 12 (1999) 285–292.

[40] S. Wang, G.M. Poon, W.D. Wilson, Quantitative investigation of protein-nucleic acid interactions by biosensor surface plasmon resonance, Methods Mol. Biol. 1334 (2015) 313–332.

[41] D.G. Myszka, Improving biosensor analysis, J. Mol. Recognit. 12 (1999) 279–284.

[42] R. Nanjunda, M. Munde, Y. Liu, W.D. Wilson, Real-time monitoring of nucleic acid interactions with biosensor-surface plasmon resonance, in: M. Wanunu, Y. Tor (Eds.), Methods for Studying Nucleic Acid/Drug Interactions, CRC Press, Boca Raton, 2011, pp. 91–122.

[43] J.R. Jenquin, L.A. Coonrod, Q.A. Silverglate, N.A. Pellitier, M.A. Hale, G. Xia, M. Nakamori, J.A. Berglund, Furamidine rescues myotonic dystrophy type I associated mis-splicing through multiple mechanism, ACS Chem. Biol. 13 (2018) 2708–2718.

[44] R. Simone, R. Balendra, T.G. Moens, E. Preza, K.M. Wilson, A. Heslegrave, N.S. Woodling, T. Niccoli, J. Gilbert-Jaramillo, S. Abdelkarim, E.L. Clayton, M. Clarke, M.T. Konrad, A.J. Nicoll, J.S. Mitchell, A. Calvo, A. Chio, H. Houlden, J.M. Polke, M.A. Ismail, C.E. Stephens, T. Vo, A.A. Farahat, W.D. Wilson, D.W. Boykin, H. Zetterberg, L. Partridge, S. Wray, G. Parkinson, S. Neidle, R. Patani, P. Fratta, A.M. Isaacs, G-quadruplex-binding small molecules ameliorate *C9orf72* FTD/ALS pathology in vitro and in vivo, EMBO Mol. Med. 10 (2018) 22–31.

[45] R.L. Rich, D.G. Myszka, Advances in surface plasmon resonance biosensor analysis, Curr. Opin. Biotechnol. 11 (2000) 54–61.